

Accepted Manuscript

Carbonate platform facies development of the turonian wata formation in central and eastern sinai, Egypt

M.A. Khalifa, S. Farouk, A.M. Hassan



PII: S1464-343X(16)30305-3

DOI: [10.1016/j.jafrearsci.2016.09.011](https://doi.org/10.1016/j.jafrearsci.2016.09.011)

Reference: AES 2669

To appear in: *Journal of African Earth Sciences*

Received Date: 21 February 2016

Revised Date: 11 September 2016

Accepted Date: 15 September 2016

Please cite this article as: Khalifa, M.A., Farouk, S., Hassan, A.M., Carbonate platform facies development of the turonian wata formation in central and eastern sinai, Egypt, *Journal of African Earth Sciences* (2016), doi: 10.1016/j.jafrearsci.2016.09.011.

This is a PDF file of an unedited manuscript that has been accepted for publication. As a service to our customers we are providing this early version of the manuscript. The manuscript will undergo copyediting, typesetting, and review of the resulting proof before it is published in its final form. Please note that during the production process errors may be discovered which could affect the content, and all legal disclaimers that apply to the journal pertain.

**CARBONATE PLATFORM FACIES DEVELOPMENT OF THE
TURONIAN WATA FORMATION IN CENTRAL AND EASTERN
SINAI, EGYPT**

M. A. Khalifa*, S. Farouk**, and A. M. Hassan***

*Geology Determent. Menoufia University, Shibben El Kom, Egypt.
kh_cycle@yahoo.co.uk

**Exploration Determent, Egyptian Petroleum Research Institute, Nasr City,
11727, Egypt. geo.sherif@hotmail.com

***Geology Determent, Sohag University, Sohag, Egypt,
geoabdallah@gmail.com

ABSTRACT

The Wata carbonate platform in central and eastern Sinai show a clear pattern of evolutionary development during sedimentation. Three facies are recognized in the carbonate platform. Inner-platform in the south, inter-platform basin in the middle, and outer-platform in the northwest. Such classification was probably performed by the effect of Syrian Arc System that culminated during Turonian in Sinai. Inner-platform includes fining-upward cycles, each begins with packstone, followed by wackestone and capped by lime-mudstone or claystone or molluscan bioclastic wackestone at the base capped by sandy oolitic packstone or dolostone. The dominant faunal associations are molluscs, and echinoids. Inter-platform basin occurs north of inner-platform and extends northwest-southeast direction and comprises fining-upward cycles, each of which begins with bioclastic ostracodal packstone, calcisphere packstone, bioclastic packstone, capped by wackestone and lime-mudstone The faunal association includes, sponge spines, ostracodes, molluscan debris and calcispheres. They were deposited in

shoal marine and barrier. The outer-platform occurs at Gebel Giddi and 31
extended northwestwards. The lithofacies are entirely represented by 32
calcsphere wackestone/packstone, with a reduced thickness of 20 m. 33

Keyword: Carbonate platform, Wata Formation, Turonian, Sinai, Egypt 34

35

1. Introduction 36

Passive margin basins are generally considered to be the major site of 37
carbonate platform formation (e.g. Wright and Burchette, 1999; Einsele, 38
1992; Bachmann and Kuss, 1998). The largest and most extensively studied 39
Cenozoic platforms come from the Florida–Bahamas region (e.g., Schlager, 40
1981 & 1999; Schlager and Ginsburg, 1981 and Ginsburg, 2001), the Great 41
Barrier Reef (e.g., Davies *et al.*, 1989) and the NW shelf of Australia 42
(Butcher, 1990). Sedimentology and stratigraphy of these platforms are 43
dominantly controlled by the low rate of sedimentation and the localization of 44
siliciclastic supply from the adjacent mature continental landscape or isolation 45
from clastic supply in offshore banks, subsidence at relatively slow rates in 46
the Cenozoic (~0.03–0.04 m/ky, from Schlager and Ginsburg, 1981) as well 47
as regional or eustatic sea-level changes. During the Cenomanian-Turonian a 48
carbonate platform which extended over large parts of northern parts of Sinai 49
was established (Bauer *et al.*, 2002). As a result of eustasy and local 50
subsidence, the sea level fluctuated over the predominantly shallow water 51
platform during the Cenomanian and Turonian leading to cyclic 52
sedimentation of a variety of sedimentary rocks. 53

Ghorab (1961) assigned the name Wata Formation for the carbonate 54
succession at Wadi Wata in western Sinai. In central and eastern Sinai, little 55
sedimentological work has been done on the Turonian Wata Formation (e.g., 56
Said, 1971; Barakat *et al.*, 1986; El Azabi and Al Araby, 1996; Bachmann 57
and Kuss, 1998; Luning *et al.*, 1998a and 1998b; Kuss *et al.*, 2000 ; Khalifa *et* 58
al., 2003; El-Hariri *et al.*, 2012). However, geological discussion on the Wata 59
Formation was done by (Issawi *et al.*, 1981; Cherif *et al.*, 1989; Kora and 60
Hamama, 1987; and Ziko *et al.*, 1993). All the above studies were focused on 61
local Turonian sections without focusing on the lateral and vertical facies 62
changes during the Turonian time. The studied localities in the present work 63
are situated at Gebel Giddi, El Mineidra El Kebira, Gebel Shiti, Gebel Gunna, 64
Gebel El Hazim and Wadi Watir in central eastern Sinai (Fig. 1). Aims of this 65
paper are 1) to describe the facies associations of the Wata Formation, 2) to 66
interpret the possible depositional environments of the studied facies, 3) to 67
document the broad stratigraphical and depositional history of the Wata 68
carbonate platform, and 4) to interpret the reasons for the development of 69
pure carbonate platform in this particular area. This approach will help in 70
understanding the dominant control on development of carbonate platform. 71

2. Geological setting 72

The Sinai Peninsula lies at the junction between Africa and Asia continents 73
and represents the Asian part of Egypt. Egypt lies in the northeast of the 74
African Plate, where it forms a part of the Sahara Craton (El Emam *et al.*, 75
1990) that is considered as a part of a passive continental margin of 76

Gondwana. During its passive margin phase, the North African margin was 77
also influenced by pulses of compression, strike-slip and extension in specific 78
areas (Guiraud *et al.*, 2001). Most notably in the Arabian-Egyptian region, the 79
margin was affected by tectonic inversion along the Syrian Arc (Garfunkel, 80
1999). Geologically, Egypt includes three structural units; the Arabian- 81
Nubian Massif in the south, southern facies belt in the central region; and the 82
northern facies belt in the extreme north. The Arabian-Nubian Shield (New- 83
Proterozoic) in the southern Western Desert, the eastern parts of the Eastern 84
Desert (Red-Sea hills) and the southern Sinai consist of gneisses, granitoids, 85
and meta-sedimentary rocks. It was formed by early evolution from the 86
accretion of island arcs (during New-Proterozoic) and of oceanic terrains 87
(Stern, 1985; Guiraud *et al.*, 2001). The Upper Cretaceous southern facies belt 88
(equivalent to stable shelf of Said, 1962) overlapped on the Arabo-Nubian 89
Massif extending in a northeast-southwest direction. It represents a platform 90
consisting mostly of the Maghrabi/Bahariya formations (Early Cenomanian); 91
El Heiz (Late Cenomanian), El Hefhuf Formation (Turonian-Santonian) and 92
Ain Giffara Formation (Campanian). The above sequence is capped by the 93
Khomani Chalk (Maastrichtian). The northern facies belt of Late Cretaceous 94
age (equivalent to the unstable shelf of Said, 1962) is coeval to the southern 95
facies belt, and was affected by the Syrian Arc System (Late Cretaceous), 96
which formed northeast-southwest trending anticlinal and synclinal structures. 97
The northern facies belt in this study comprises the Galala/Raha formations 98
(Cenomanian), Abu Qada Formation (Cenomanian-Turonian), Wata 99

Formation (Turonian), Matulla Formation (Campanian) and the Sudr Chalk 100
(Maastrichtian). The Hercynian Orogeny affected the southern facies belts, 101
where it retarded the deposition of Silurian, Devonian, Carboniferous, 102
Permian, Triassic, and Jurassic rocks. This made a prolonged hiatus between 103
the top of the Naqus Formation and the Lower Cretaceous Malha Formation 104
(422.9- 99.5 Ma). The Laramide Revolution occurred between the Lower 105
Cretaceous Malha Formation and the Cenomanian Galala Formation, making 106
a wide gap or hiatus starting from 112 to 99.6 Ma. Also, the Hercynian 107
Orogeny affected the northern facies belts. This made a prolonged hiatus 108
between the top of the Naqus Formation and the Lower Cretaceous Malha 109
Formation (422.9-112 Ma). The Syrian Arc System can be traced from Syria 110
to the central Western Desert of Egypt, via Sinai and the northern part of the 111
Eastern Desert (Kuss et al., 2000). Folding of the Syrian Arc System began in 112
post-Cenomanian times and reached its acme during the Late Cretaceous (Aal 113
and Lelek, 1994; Farouk and Faris, 2012; Farouk et al, 2014). Hence, the 114
Turonian rocks were deposited on the paleotopography of the structural highs 115
and lows in central and eastern Sinai. This affected on the facies type of the 116
Turonian Wata Formation both laterally and vertically. At Gebel Shiti, Gebel 117
Gunna, and Wadi Watir, the contact between the Abu Qada and the Wata 118
formations is unconformable and is placed between the claystone of the 119
topmost Abu Qada Formation and the limestone containing bivalves and 120
planktonic foraminifera of basal Wata Formation. At Gebel El Hazim, the 121
contact is unconformable and is placed between the brown sandstone of the 122

topmost part of the Abu Qada Formation and the yellowish white limestone 123
with chert bands of the basal Wata Formation (Fig. 2). At Gebel Giddi and El 124
Mineidra El Kebira the Wata Formation conformably overlies the Early 125
Turonian Abu Qada Formation. At the first locality, this contact is placed 126
between the yellowish grey limestone of the uppermost Abu Qada Formation 127
and the white chalky limestone with chert nodules in the basal part of the 128
Wata Formation. The upper contact of the Wata Formation at Gebel Shiti, 129
Gebel El Hazim and Wadi Watir is unconformable and lies between the pale 130
yellow limestone with chert bands of the topmost Wata Formation and the 131
green claystone of the basal Matulla Formation. At Gebel Gunna, the same 132
upper contact is placed between the cherty limestone of uppermost part of the 133
Wata Formation and the dolomite of the basal Matulla Formation (Fig. 2). 134
Lithologically, the Wata Formation at Gebel Giddi consists of chalky 135
limestone enriched with ammonites and molluscan shell fragments and 136
measures about 28 m in thickness. At El Mineidra El Kebira, this formation is 137
made up of marly limestone intercalated with marls and claystone and 138
assumes about 93.5 m in thickness (Fig. 3A). The limestone is enriched with 139
gastropods, brachiopods, algae, corals, sponges and echinoids (Fig. 3B). 140
Southeastwards, the Wata Formation outcrops and forms the cap of El Tih 141
escarpment such as at Gebel Shiti and Gebel Gunna assuming about 35 m in 142
thickness. This formation increases in thickness further northeast at Gebel El 143
Hazim and Wadi Watir reaching up to 100 m (Fig. 2). At the latter localities 144
the Wata Formation comprises of hard thick to thin bedded limestone and 145

dolostone with occasionally marl layers (Fig. 3C). Few clay and sandstone are 146
intercalated with the limestones. The marl beds are fossiliferous with 147
ammonites and molluscan shell fragments. 148

The Wata Formation contains several benthic foraminifera marker for the 149
Late Turonian age, among which are *Discorbis turonicus* Said & Kenawy, *D.* 150
minutus Said & Kenawy and *Eponides lotus* (Schwager). It also yielded rare 151
and sporadic planktonic foraminifera such as, *Hedbergella delrioensis* Carsey, 152
H. simplex Morrow, *H. planispira* (Tappan) *Whiteinella archaeocretacea* 153
Pessagno, *Whiteinella baltica* Douglas & Rankin, *W. inornata* (Bolli) and 154
Heterohelix moremani (Cushman). The first appearance of the *Discorbis* 155
turonicus during the Late Turonian has been accepted by several previous 156
workers in Egypt (e.g., El Shinnawi and Sultan, 1972; Andrawis, 1990; 157
Shahin and Kora, 1991; Ismail, 2000; Samuel *et al.*, 2009). In addition to, the 158
Upper Turonian zonal index ammonite *Coilopoceras requienianum* 159
(D'Orbigny) has been found in the Wata Formation. In east central Sinai, the 160
Wata Formation is assigned to the Middle-Late Turonian due to the 161
occurrence of the calcareous nannofossils CC 12 Zone (Bauer *et al.*, 2001, 162
2003; Farouk, 2015; Farouk *et al.*, 2016). 163

3. Methods 164

To delineate the nature of the lower and upper contacts of the Wata 165
Formation with the overjacent and subjacent rock units, six stratigraphic 166
sections have been measured at Gebel Giddi, El Mineidra El Kebira, Gebel 167
Shiti, Gebel Gunna, Gebel El Hazim and Wadi Watir (Figs. 1,2). The rock 168

samples have been studied in thin sections under petrographic microscope. 169

Micro- and macro faunal associations were identified from this rock unit to 170

delineate its biozone and exact age. The measured sections have been 171

correlated on the basis of the ammonite fossils and lithological characteristics. 172

4. Facies analysis 173

The petrographic investigation on the Wata Formation revealed the presence 174

of several lithofacies represented by lime-mudstone, molluscan bioclastic 175

wackestone, ostracodal wackestone, foraminiferal wackestone, pelletal 176

foraminiferal packstone, sandy oolitic molluscan packstone, calcispheres 177

packstone, dolosparite, dolomicrite, quartzarenite and claystone (Fig. 2). 178

4.1 - Lime-mudstone (LM) 179

The lime-mudstone lithofacies is common in the Wata Formation. At Wadi 180

Watir, it forms a thick horizon near the topmost part of the Wata Formation 181

with a thickness of 12.0 m. At Wadi Hegni (Gebel El Hazim) and Gebel Shiti 182

the lime-mudstone is common and represented by three beds, each of which 183

does not exceed 6.5 m in thickness (Fig. 2). At Gebel Gunna, this lithofacies 184

is reduced in thickness, and is represented by 2.0 m thick near the middle part 185

of the formation. It is also present at El Mineidra El Kebira, where it is 186

intercalated with the calcispheres and ostracodal packstones (Fig. 2). This 187

lithofacies consists of fine dense and dark grey microcrystalline calcite and 188

contains rare foraminiferal skeletal particles floating in the dense lime mud. 189

Such facies are completely obliterated by aggrading neomorphism into 190

microsparry calcite (Fig.4A). Also, the lime mud shows slight degree of 191
recrystallization into xenotopic microspar (10 um) and dolomitized in parts. 192

Interpretation: the lime-mudstone was deposited in calm water due to the 193
absence of variable amount of skeletal particles. Most of lime mud may be 194
derived from the abrasion and micritization of the skeletal particle especially 195
in the restricted areas. The microspar was originally deposited as micrite with 196
associated clay minerals, as well as the rare skeletal particles, suggesting that 197
this lithofacies was deposited in a subtidal or low ramp environment below 198
wave base (Calvet and Tucker, 1988). Within argillite layers the skeletal 199
material lies parallel to the bedding suggesting slow sedimentation rates 200
(Elrick and Read, 1991). This facies is devoid of indigenous benthonic fauna 201
or burrows suggesting anoxic conditions during deposition (Marquis and 202
Laury, 1989). The absence of wave and current-induced structures suggests a 203
subtidal environment below storm wave base (Keller, 1997). 204

4.2- Molluscan bioclastic wackestone (MBW) 206

The molluscan bioclastic wackestone forms the topmost part of the Wata 207
Formation at El-Tih escarpment and Gebel Gunna with a thickness of about 208
4.0 m, and 20.0 m respectively. At Wadi Watir, it is about 11.0 m thick near 209
the lowermost part of the sequence, each bed ranges in thickness from 3 to 8 210
m thick (Fig. 2).It is enriched with bivalves and different skeletal debris. 211
Petrographically, it is made of sorted molluscan particles forming about 80% 212
of the rock and shows preferred orientation parallel to the bedding plane. 213

Most of the molluscan particles exhibit aggrading neomorphism from their 214
centers and are coated with micrite envelopes (Fig. 4B). The micritic matrix 215
became granular as well as mosaic sparry calcite in parts. Rock particles are 216
mainly molluscan shell fragments and bioclastic grains. 217

Interpretation: Bivalves rich skeletal assemblages are widely recorded in 218
modern non-tropical carbonate sediments on the Wanganui shelf off central 219
western New Zealand (Gillespie et al., 1992). The assemblage is often best 220
represented in areas with relatively higher sedimentation rate of fine 221
terrigenous material, less favored by many of the other skeletal contributors, 222
and often associated with shallower-shelf waters (Nelson *et al.*, 1988). 223

4.3- Ostracodal wackestone (OW) 224

This lithofacies is recorded in the Wata Formation at Gebel Gunna and Wadi 225
Watir assuming a thickness of 10.5 m and 12.0 m respectively. It also occurs 226
at El Mineidra El Kebira intercalated with calcispheres 227
packstone/wackestone. Rocks of this lithofacies are yellowish brown to 228
creamy in colour, hard and are characterized by a papery or thinly laminated 229
appearance. Petrographic investigation revealed that the rock is made up of 230
dark grey dense micrite matrix rich with thin bivalve shells that are composed 231
of calcite with a radial fibrous structure. Ostracodes are scattered randomly in 232
the lime matrix (Fig. 4C). Rare foraminiferal tests are also recorded 233
disseminated in the matrix and show microspar filling the whole tests as a 234
result of aggrading recrystallization (Fig. 4C). Few clear dolomite rhombs are 235
also observed within the lime mud matrix. They are idiotopic with 236

unequigranular fabric and range in size from 0.02 to 0.05 mm. Also, few pores and vugs are more or less filled with coarse mosaic spar as cement.

Interpretation: Bioturbated mudstones and wackestones with moderate fossil diversity (ostracodes, pelecypods, gastropods, miliolids, other benthic foraminifera, dasycladaceans, and sponge spicules) are attributed to semi-restricted lagoons (Colombie and Strasser, 2005). Faunal diversity is low and normal marine fauna are lacking, except for ostracode shells, calciphores and dasycladacean algae, which indicate quiet, sheltered conditions such as a lagoonal environment (Khalifa and Zaghoul, 1990). Zoophycos burrows indicate deep subtidal conditions. Similar facies elsewhere in the geological record have been interpreted as low energy sub-wave base deposits (Markello and Read, 1981).

4.4- Foraminiferal wackestone (FW)

Foraminiferal wackestone occurs at El Minediara El-Kebiara. It occurs also at the middle part of the Wata Formation in both Wadi Watir and Wadi Hegni (Gebel Hazim) where it attains a thickness of about 20 m, and 12 m respectively. It is composed of yellowish brown limestone, very hard, massive with some chert nodules. This lithofacies is made essentially of skeletal particles closely packed in a dark dense micrite matrix. Skeletal particles are represented by foraminiferal tests (e.g. miliolide, nodosaria, textularia) and some bioclastic grains (Fig.4D). Foraminiferal tests are represented by benthonic type and forming about 30% of the rock. Some of these tests are susceptible to change to microspar by aggrading neomorphism while their

internal structure is still well preserved. Bioclastic grains account about 5% of 260
the rock. They are represented mainly by ostracodal valves with curved shape 261
and size up to 0.20 mm (Fig.4D). Other elongated bioclastic grains, which 262
refers to molluscan particles, are also encountered. They are replaced by 263
mosaic sparry calcite with straight intercrystalline boundaries with a size of 264
about 0.04 mm (Fig. 4D). 265

Interpretation: The common presence of benthonic foraminifera, e.g. 266
miliolide indicates restricted water condition. It usually occurs in shallow 267
water and back reef lagoon (Henson, 1950). Moreover, Wilson (1975) has 268
found that miliolide are the most common foraminiferal particles representing 269
the shallow restricted lagoon environments. This lithofacies was deposited in 270
deeper subtidal conditions. The presence of mud-supported texture, and the 271
apparent absence of wave and current structures, suggests that this facies was 272
deposited in a low energy environment below normal wave base (Calvet and 273
Tucker, 1988; Tucker and Wright, 1990). The faunal diversity indicates a 274
stable open marine environment at moderate depth, characterized by the 275
accumulation of foraminifera and molluscan debris. 276

4.5- Pelletal foraminiferal packstone (PFP) 278

The pelletal foraminiferal packstone lithofacies has a wide distribution 279
throughout the Wata Formation. It is represented by two horizons at Gebel 280
Shiti with a total thickness of 9.m. At Gebel Gunna, this lithofacies occurs at 281
the lower part of the Wata Formation with a thickness which ranges from 2.0 282

to 9.0 m. Rocks belonging to this lithofacies are whitish gray to creamy in colour, well-bedded, hard and characterized by comb structure in parts. In thin section, this lithofacies is essentially made up of well rounded micritic pellets that originate from the extensive micritization of the foraminiferal tests. They are well rounded, sorted, vary in size from 0.20 to 0.30 mm and are cemented by microspar which forms the other foraminiferal tests (Fig. 5A). Foraminifera are represented by benthonic forms such as miliolide and ostracodes. Most of the miliolide and ostracodes were extensively micritized to the extent that the whole particles change to dull dark grey, looks like, pellets. Moreover, some relics of the miliolide still occur (Fig. 5A). They are rounded in shape and have a size of about 0.30 mm. Rare bioclastic grains as well as crinoid plates also occurs.

Interpretation: The pelleted foraminiferal wackestone that contains a more restricted miliolides and ostracodes indicates brackish water environment (Mack and James, 1986). The predominance of micrite in between particles reflects quiet water condition.

4.6- Sandy oolitic molluscan packstone (SOMP)

The sandy oolitic molluscan packstone is encountered at the lower part of the Wata Formation both at Wadi Watir and Wadi Hegni (Gebel Hazim) with a total thickness of about 21 m (Fig. 2) Rocks belonging to this lithofacies are light grey to yellowish grey in colour, medium-grained, hard, rich with molluscan shell debris, and characterized by large scale cross-bedding at

Wadi Watir. The rock is made essentially of coarse oolitic skeletal particles 306
and detrital quartz grains packed in a coarse mosaic matrix (Fig.5B). Oolites 307
account for about 15% of the rock with a size reaching 0.50 mm in diameter. 308
Some of these oolites suffer aggrading neomorphism to pseudospire starting 309
from the core. Skeletal particles account for about 30% of the rock and are 310
represented by molluscs, echinoids, foraminiferal tests and algae with rare 311
bryozoan fragments (Fig.5B). Molluscan shell walls were replaced by 312
pseudospire as a result of aggrading neomorphism. In addition, some of them 313
show micrite envelopes around their shells as a result of algal borings. Few 314
shell debris of the molluscan grains are subjected to silicification, i.e., 315
cryptocrystalline silica replaced the original shell of the oyster fragments. Fine 316
to coarse-grained detrital quartz grains make 15 % of the rock. These grains 317
show clear diagenetic feature where the grain peripheries are replaced with 318
calcite. Granular spire crystals as well as drusy calcite are acting as cement 319
while the massive spar that represents secondary cement, may be resulted 320
from the recrystallization of the original lime mud (Fig. 5B). 321

Interpretation: The sandy oolitic molluscan packstone grainstone was 322
probably deposited in current or wave-agitated shallow subtidal environments 323
(Osleger and Read, 1991). The highly diversity of allochems (echinoids, 324
bryozoa, mollusca, peloids, ooids and intraclasts) embedded in a sparry 325
calcite cement, point to an influence of shallower and more agitated water, 326
probably shoal area (Wilson, 1975 and Flugel, 1982). The association of 327
peloids, intraclasts and oolites reflects restricted shoal deposits with moderate 328

to high circulation (Luning *et al.*, 1998a). The oolitic-intraclastic grainstone is deposited in agitated, shallow subtidal water as low-relief shoal (Tucker *et al.*, 1993).

4.7 - Calcisphere packstone (CP)

This lithofacies occurs in the Wata Formation at El Giddi area. The rock is yellowish white in colour with thickness of 24 m. The rock consists of calcispheres (35%), bioclasts (15%), algae (3%) echinoid spines (2%) and lime mud matrix (Fig.5C). Calcispheres are common, and show a concentric wall structure. Bioclasts are most probably derived from algal skeletons. Few algal fragments are observed and are represented by coated grains (oncolites). Their internal cells are filled with micrite. The embedding material is a lime mud matrix (45%) and shows thin laminations and containing few empty pores (Fig. 5C).

Interpretation: The calcispheres assemblage is most typical of off-shelf waters where turbulence is minimal, allowing the pelagic settling and accumulation of planktonic foraminifera-rich ooze (Hayton *et al.*, 1995; El-Azabi and Farouk, 2011). This assemblage may occur at shallow depths in partly enclosed basins where low-energy zones develop at the end of current paths as found in Bass Basin, southeastern Australia (Blom and Alsop, 1988). The presence of oncolite indicates restricted marine water or lagoon (Peryt, 1977). However, a literature overview suggests that two environments were the main habitat of calcispheres, i.e. shallow water sheltered

environments and an open marine realm. Calcispheres indicate well - 352
sheltered, very shallow water such as lagoonal, back reef (Marszalek, 1975; 353
Kaźmierczak, 1975 and 1976). 354

4.8- Dolosparite (DSS) 355

In the Wata Formation, this lithofacies is represented by three horizons that 356
occur between the pelletal foraminiferal packstone lithofacies at Gebel Shiti . 357
Each horizon has a thickness of about 1.50 m. It also occurs at Gebel Hazim 358
(Wadi Hegni) with an average thickness of 5 m. Rocks belonging to this 359
lithofacies are greyish yellow to dark brown, hard, burrowed. The rock mainly 360
consists of well-defined dolomite rhombs (90-95%) and some unfilled pore 361
spaces. The matrix is mosaic sparry calcite with a size ranging from 0.16 to 362
0.24 mm. Most of the dolomite rhombs are of medium-grained (0.08 mm) and 363
show hypidiotopic to xenotopic fabric and equigranular texture (Fig. 5D). 364
They are of rich inclusion type where they contain thin threads of ferric 365
hydroxide along the rhombohedral cleavage. Vugs and pores are mostly 366
unfilled while rare of them are filled with rounded to subrounded chert 367
nodules with size of about 0.8-0.16 mm. These filled pores that originally 368
may be formed due to burrowing organisms were filled with cryptocrystalline 369
silica. 370

Interpretation: This type of coarse-grained dolostone suggests later phase of 371
dolomitization, since the coarse dolomite rhombs are usually need long period 372
of time to be formed. This dolomite facies is interpreted to represent an 373
intermediate to late-diagenetic replacement dolomite. The coarse crystal size 374

suggests a major, probably long lasting, dolomitization event. Cloudy cores 375
represent replacive dolomite, whereas the clear rims are zoned dolomite 376
cements that occlude intercrystalline porosity (Lohmann and Meyers, 1977 377
and Amthor and Friedman, 1991). This type includes dolomite cement and 378
dolomite replacing precursor cement. This dolomite type occurs together with 379
fine crystalline dolomite types. Paragenetic relationships indicate that coarse 380
crystalline dolomite is later than fine crystalline dolomite (Khalifa and Abu 381
El-Hassan, 1993) and contemporaneous (replacive dolomite). Coarse- 382
crystalline dolomites may occur as a replacement of limestone during late 383
diagenesis in the deep subsurface (Machel and Anderson, 1989) and this 384
process may be controlled by the coarse-grained texture of the original 385
deposits that are being replaced during late diagenesis (Folk and Land, 1975; 386
Sibley et al., 1993). 387

4.9- Dolomicrite (DM) 388

In the Wata Formation, the dolomicrite occurs only at Wadi Hegni (Gebel El 390
Hazim) it is faint yellowish in color, thinly bedded with rare shell debris and 391
measures about 10 m in thickness. Microscopically, the rock of this 392
lithofacies consists mainly of very fine dolomite rhombs (70-80%), as well as 393
some detrital quartz grains. Dolomite rhombs are usually hypidiotopic to 394
xenotopic with equigranular texture (Fig.6A). They range in size from 8 to 15 395
um and are mostly of inclusion rich type along the rhombohedral cleavage, as 396

well as they are lacking zoning. Some unfilled vugs and pore spaces with a size of 0.20 mm in diameter are also recorded.

Interpretation: In many cases dolomicrite can form shortly after deposition or as an early-stage replacement mineral in modern supratidal and shallow intertidal environments as found in the Recent sediments in Arabian Gulf (Friedman, 1968; Shinn et al., 1965; Shinn, 1983). The presence of this facies within the carbonate facies reflect the lowering in sea level during sedimentation that permit the slight evaporation and consequent dolomitization (Folk and Land, 1975).

4.10- Quartzarenite (QA)

In the Wata Formation, the quartzarenite lithofacies lies in the middle part between the sandy oolitic packstone lithofacies at Wadi Watir (Fig. 6B). In thin sections, the rock consists of well sorted quartz grains accounting 95% of the rock with rare feldspar grains and carbonate rock fragments. The quartz grains are medium- to coarse-grained, well rounded, Clay matrix is rarely recorded as very fine dull grains. Quartz grains are rounded and highly compacted with tangential and suture contacts. They range in size from 0.2 to 0.4 mm in diameter. Most of the grains are highly mature and coated with dark ferruginous material as thin films (Fig.6B). The cementing materials are represented essentially by silica overgrowths that form an equal envelopment around the original quartz grains. The silica overgrowths are separated by ferric oxide.

Interpretation: The quartzarenite that is well sorted may be deposited on the shore as dune and beach sands and may include near shore littoral sand. Also, quartzarenite can be found in the intertidal zone. The presence of silica overgrowths as cement indicates subaerial exposure of the sandstone and or deposition in continental environment ,since most of the silica overgrowths in sandstones is considered second phase of cementation as evidenced by the presence of iron oxides coating around quartz grains. This phenomenon was described in the quartzarenites that bound the depositional sequences in fluvial and fluviomarine facies (Salem *et al.*, 1998 and Abdel Wahab *et al.*, 1998). The northward thinning of the quartzarenite reflects the proximity of this facies to terrigenous provenance south and eastwards peripheries of basin.

4.11- Claystone lithofacies (CL)

Claystone lithofacies is recorded only in the middle and upper parts of Gebel Shiti in east central Sinai (Fig.2). In the later locality it forms the base of the second cycle and the middle part of the last cycle. It has a thickness varying from 3.0 to 9.0 m. The rock is yellowish gray in colour, highly with thin laminae of gypsum as well as thin bands of ferruginated sandstone (quartzwacke).

Interpretation: The deposition of claystone may be occurred during rapid settling from suspension probably as consequence of clay flocculating from concentrated suspension (Potter *et al.*, 1980) .The claystone can be transported from cratonic area nearby the basin during subsidence or increase in sea level (Osleger and Read, 1991).

5. Discussion	442
The Wata carbonate platform in central and eastern Sinai show transitional	443
facies changes from southeast to northwest and can be classified into three	444
coeval environments. These are: inner-platform in the southeast, inter-	445
platform basin in the middle and outer platform in the northwest (Fig. 7A).	446
This opinion is contradicted with Wilmsen and Nagm (2012) who considered	447
that the depositional setting of the Cenomanian and Turonian in the southern	448
Galala plateau as a homoclinal carbonate ramp. This classification is similar	449
to the opinion of Bauer et al. (2002) during their study of Turonian Wata	450
Formation in Sinai. The subdivision of the carbonate platform was affected	451
probably by the Syrian Arc System that was active during the Late Cretaceous	452
(Shahar, 1994; Walley, 1998). In Sinai, "Early Alpine" transgression since the	453
Turonian resulted in the structural inversion of older half grabens (Moustafa	454
and Khalil, 1990).	455
The inner-platform includes Gebel Shiti, Gebel Gunna, Gebel El Hazim	456
(Wadi Hegni) and Wadi Watir. The most pronounced facies associations are	457
represented by lime-mudstone, dolosparite, dolomicrite, ostracodal	458
wackestone, molluscan bioclastic packstone, sandy oolitic molluscan	459
packstone and quartzarenite. Such facies were probably deposited in shallow	460
subtidal to intertidal environments. These lithofacies show vertical	461
arrangement in the form of fining-upward cycles. Each cycle commences with	462
sandy oolitic molluscan packstone, followed upward either by molluscan	463
bioclastic wackestone and capped by lime-mudstone, or molluscan bioclastic	464

wackestone, capped by lime-mudstone. The vertical arrangement of such cycles that show fining-upward cycles indicates subsidence during sedimentation. This may represent the foundation stage of platform formation (Szulezewski *et al.*, 1996). The presence of coarse-grained and fine-grained dolomite in the inner platform indicate vibration in sea-level between intertidal to supratidal during sedimentation. The formation of dolomite needs shallowing water and sea-level fall to enable dolomitization process to be performed while the carbonate lithofacies indicate high-stand sea-level (Bauer *et al.*, 2002). At Wadi Watir, the oolitic packstone was accumulated vertically forming the lower half of the sequence. Subsequent to the oolitic facies, the quartzarenite facies was accumulated above the oolitic facies. Their deposition was occurred in shallow subtidal to intertidal zone (Klein, 1970). The quartz grains were derived from the exposed basement rocks in southeastern side of the basin. The oolitic and quartzarenite lithofacies were deposited in high agitation water in shoal marine representing a barrier. Such a barrier may represent the transition from the inner platform to inter-platform setting (Figs. 7A&7B). However, sediment transport, coarse-grained carbonates, and oolitic shoals are generally common on platforms during highstand (James and Kendall, 1992).

The inter-platform basin occurs north of the inner-platform (Fig. 7A) and occurs at El Mineidra El Kebira. In such restricted basins, the lithofacies have an average thickness of 93 m. In the inter-platform basin, the carbonate succession comprises fining-upward cycles, each of which begins with

bioclastic ostracodal packstone, bioclastic packstone, capped by wackestone 488
and lime-mudstone. Such facies associations reflect increased carbonate 489
production rates. Such fining-upward cycles may indicate local structural 490
control such as continuous subsidence during sedimentation. The packstones 491
were deposited in shallow warm condition near the wave base, when 492
subsidence started the water condition was changed (depth, salinity, wave 493
action....etc.) which permit the sedimentation of wackestone and lime- 494
mudstone. The presence of miliolids, ostracode suggests sheltered and quiet 495
water condition (Wilson, 1975). 496

The outer-platform occurs at Gebel Giddi and is extended farther northwards 497
(Figs. 7A&7B). The lithofacies are entirely represented by calcisphere 498
wackestone/packstone, with a reduced thickness of 20 m (Fig. 2). The outer 499
platform facies is made up of different lithofacies (e.g.calcisphere 500
wackestone/packstone) that widely differ from the inner and inter-platform 501
facies. The hemipelagic calcisphere wackestone/packstone facies contains 502
decimeter-scale bedding and are arranged in 05- to 40 cm thick beds that are 503
massive, bioturbated and lack evidence of cyclicity. Contacts between beds 504
are sharp and conformable. These lithofacies were deposited from suspension 505
(hemipelagic facies) and transported down slope by gravity. This is similar to 506
the platform margin south-central Pyrenees, Spain (Drzewiecki and Simo, 507
2000). The thickness of the outer-platform reaches up to 93 m, more or less, 508
three times than the inner- and inter-platform. This indicates that the rate of 509
subsidence in the outer-platform is greater than inner- and inter-platforms. 510

These subsidence events in each section seem to have been approximately 511
simultaneous through the entire area, although they can have very different 512
responses in each section. For example, a major subsidence event can be 513
recognized in all sections in the Late Cenomanian, but the local consequences 514
of that event were very different: even causing the drowning of the previous 515
shallow platform, whereas in others was the opposite, causing their uplift and 516
emersion. 517

Calcispheres are usually denoted as hollow, spherical calcareous microfossils 518
of various origins. Some calcispheres were interpreted *e.g.* as being 519
representatives of volvocacean algae (Każmierczak, 1976), reproductive cysts 520
of dasycladacean green algae (Marszalek, 1975), radiolarians (Antoshkina, 521
2006), or post-mortem calcified acritarchs (Każmierczak and Kremer, 2005). 522
Many of the Mesozoic and Cenozoic calcispheres are now considered to be 523
calcareous dinoflagellate cysts (Keupp, 1981). As already pointed out by 524
Flügel (2004) and indicated by the above listed authors, calcispheres 525
occurring in an open marine realm mostly represent calcareous 526
dinoflagellates, or organisms related to them, and are most frequently reported 527
from Mesozoic rocks, whereas pre-Mesozoic calcispheres seem to be 528
restricted to shallow-water environments. 529

6. Deepening platform 530

Basically, the deepening platform of the Wata Formation is based on cycle 531
thickness, type of cycle, variable sedimentation rates, incomplete shallowing 532
to sea-level, and unconformities. The cycle thickness will explain to some 533

extent the accommodation space; the thick cycle may indicate increase in 534
accommodation space and high rate of subsidence, while thin cycle indicates 535
decrease in accommodation space. These phenomena can be explained by 536
Fischer plots that they are conventionally drawn by cumulative departure from 537
mean cycle thickness against cycle number (no less than 50) (e.g., Sadler et 538
al., 1993). In this way, thick cycle packages positively deviate from the mean 539
cycle thickness, and form the rising limbs of the plots, reflecting a long-term 540
increase in accommodation space; whereas thin cycle packages negatively 541
deviate from the average cycle thickness, and form the falling limbs, 542
reflecting a long-term decrease in accommodation space. 543

The type of the cycles in the studied carbonate sequence in platform in the 544
measured sections can explain the deepening platform. The cycles in the 545
measured sections show fining-upward, some cycles begin with packstone and 546
capped by wackestone or lime-mudstone. Such type of cycles were described 547
by Khalifa (1996) as submergence cycles, i. e., the cycle begins with 548
deposition of packstones in shallow water, then followed upward by 549
subsidence that may resulted in the deposition of fine-grained facies and /or 550
deep water carbonate (wackestone). Incomplete shallowing of sea-level may 551
suggest the continuous subsidence during sedimentation process, even 552
lowering in sea-level, but it did not track the rate of subsidence. 553

Another important point is the time represented by unconformities. In the 554
platform under study, there are no erosional surfaces through the succession. 555
However, the stratigraphic gaps of the unconformities at the base (intra late 556

Albian) and the top (intra middle Cenomanian) of the sequence set are 557
substantial, and can be considered in the analysis. As the hiatus represented in 558
these two surfaces are below the resolution of the biostratigraphy, we 559
estimated a corresponding minimum time interval of 0.4 my. However, this 560
value is tentative. Nevertheless, since the unconformities lie below and above 561
the stratigraphic successions considered, possible modification of the hiatus 562
estimates does not notably modify the results of the analysis. This point needs 563
to be considered when comparing these results with those published for other 564
basins. 565

The contact between the Cenomanian and Turonian rocks is unconformable 566
that may be resulted from the non-deposition along a certain period of time 567
between them. This is evidenced by the absence of the Late Cenomanian– 568
Early Turonian *Mammites nodosoides* Zone (Bartov *et al.*, 1980) or creating a 569
stratigraphic gap in Sinai and Eastern Desert of Egypt (Bauer *et al.*, 2003; 570
Farouk, 2015). A stratigraphic gap occurs across the C/T boundary in large 571
parts of Sinai, apart from slope and basin deposits in the subsurface of 572
northernmost Sinai (Jenkins, 1990). In north Sinai, this gap is probably 573
related to submarine non-deposition or exposure on isolated highs, which 574
reflect the initial pulses of the Syrian Arc movements (Bartov *et al.*, 1980; 575
Kuss *et al.*, 2000). 576

Moreover, platform drowning is reflected by the rapid deepening of the 577
depositional system during the post-CeSin 7 TST and possibly also influenced 578
the genesis of the stratigraphic gap, as drowned carbonate platforms are often 579

characterized by extreme condensation or long hiatuses (Schlager, 1999). For 580
example, platform drowning across the C/T boundary in sequence boundary 581
Sb5 was associated with a long stratigraphic gap in the Lower Turonian 582
Watinoceras coloradoense Zone (Philip and Airaud-Crumiere, 1991 and 583
Philip et al., 1998). As in Sinai, this gap was followed by condensed deposits 584
in the *Mammites nodosoides* zone during the TST, and the establishment of a 585
new platform in the middle Turonian HST (Philip and Airaud-Crumiere, 586
1991). In the Pyrenees, a shorter interval of strong condensation and a 587
stratigraphic gap in the Early Turonian were also caused by platform 588
drowning (Drzewiecki and Simo, 1997). In this context, it cannot be excluded 589
that drowning in Sinai started before the onset of the post-CeSin 7 TST 590
deposits, and the stratigraphic gap may possibly be related to the drowning 591
phase. 592

7. Conclusions 593

Detailed studies of facies and facies associations of the Turonian Wata 594
Formation in central Sinai revealed the presence of three coeval carbonate 595
platform environments: the inner-platform in the southeast, inter-platform in 596
the middle and outer-platform towards the northwest. The inner-platform 597
lithofacies occurs at Gebel Shiti, Gebel Gunna, Gebel El Hazim and Wadi 598
Watir. The most pronounced facies associations are represented by lime- 599
mudstone, dolosparite, dolomicrite, ostracodal wackestone, molluscan 600
bioclastic packstone, sandy oolitic molluscan packstone and quartzarenite. 601
Such facies were probably deposited in shallow subtidal to intertidal 602

environments. These lithofacies show vertical arrangement in the form of 603
fining-upward cycles. Each cycle commences with sandy oolitic molluscan 604
packstone at base, followed upward by molluscan bioclastic wackestone and 605
capped by lime-mudstone, or molluscan bioclastic wackestone and capped by 606
lime-mudstone. 607

The inter-platform basin occurs north of the inner-platform and occurs at El 608
Mineidra El Kebira. The carbonate succession in such basin comprises fining- 609
upward cycles, each of which begins with bioclastic ostracodal packstone, 610
bioclastic packstone, capped by wackestone and lime-mudstone. Such fining- 611
upward cycles may indicate local structural control such as continuous 612
subsidence during sedimentation. The outer-platform basin occurs north of 613
the inner-platform and occurs at Gebel Giddi. The outer-platform comprises 614
of entirely of calcisphere wackestone/packstone without remarked cyclicity. 615

References 616

- Aal, A. A., Lelek, J. J., 1994. Structural development of the Northern Sinai, 617
Egypt and its implications on the hydrocarbon prospectivity of the Mesozoic. 618
In: Al-Husseini, M. I. (Ed.), Middle East Geoscience Conference, GEO'94. 619
Gulf Petrolink, Bahrain, *GeoArabia* 1, 15–30. 620
- Abdel Wahab, A., Salem, A. M. K., McBride, E. F., 1998. Quartz cement of 621
meteoric origin in silcrete and nonsilcrete sandstones, Lower Carboniferous, 622
western Sinai, Egypt. *Journal African Earth Sciences* 27, 277-290. 623
- Amthor, I. E. and Friedman, G. M., 1991. Dolomite-rock textures and 624
secondary porosity development in Ellenburger Group carbonates (Lower 625

- Ordovician), west Texas and southern New Mexico: *Sedimentology* 38, 343- 626
362. 627
- Andrawis, S. F., 1990. Tables of foraminifera biozones. In Said, R. (Ed.), *The* 628
Geology of Egypt. Balkema, Rotterdam, pp. 639-648. 629
- Antoshkina, A. I. 2006. Palaeoenvironmental implications of 630
Palaeomicrocodium in Upper Devonian microbial mounds of the Chernyshev 631
Swell, Timan-northern Ural Region , *Facies* 52, 611-625. 632
- Bachmann. M. ; Kuss, J., 1998. The Middle Cretaceous carbonate ramp of the 633
northern Sinai: sequence stratigraphy and facies distribution.- In: Wright. V. 634
P. and Burchette. T. P (Eds.) *Carbonate Ramps*.- Geological Society London, 635
Special Publication 149, 253-280, Oxford (Blackwell). 636
- Barakat, M. G., Darwish, M., El-Barkooky, A. N. ,1986. Lithostratigraphy of 637
the post-Carboniferous- pre-Cenomanian clastics in West Central Sinai and 638
Gulf of Suez, Egypt. Eighth Exploration Conference of first oil well. 17-23. 639
- Bartov, Y., Lewy, Z., Steinitz, G., Zak, I., 1980. Mesozoic and Tertiary 640
stratigraphy, paleogeography and structural history of the Gebel Areif en 641
Naqa area, eastern Sinai. *Israel Journal Earth Sciences* 29, 114–139. 642
- Bauer J., Marzouk, A., Steuber, T., Kuss, J., 2001. Lithostratigraphy and 643
biostratigraphy of the Cenomanian—Santonian strata of Sinai, Egypt. 644
Cretaceous Research 22, 497–526 645
- Bauer, J., Kuss, J., Steuber, T. 2002. Platform Environments, Microfacies and 646
Systems Tracts of the Upper Cenomanian - Lower Santonian of Sinai, Egypt. 647
Facies 47, 1-26 648

- Bauer, J., Kuss, J., Steuber, T., 2003. Sequence architecture and carbonate platform configuration (Late Cenomanian–Santonian), Sinai, Egypt. *Sedimentology* 50, 387- 414.
- Blom, W. M., Alsop, D. B., 1988. Carbonate mud sedimentation on a temperate shelf. Bass Basin, southeastern Australia. *Sedimentary Geology* 60, 269-280.
- Butcher B. P., 1990. Northwest shelf of Australia. In: Edwards J. D., Santogrossi P. A. (Eds.), *Divergent/passive margin basins*. American Association Petroleum Geologists Memoir 48, 81– 115.
- Calvet, E., Tucker, M., 1988. Outer ramp cycles in the Upper Muschelkalk of the Catalan Basin, northeast Spain. *Sedimentary Geology* 57, 785–798.
- Cherif, O. H., Al Rifaey, I. A., Al Afifi, F. I, Orabi, H. O., 1989. Foraminiferal biostratigraphy and Paleocology of some Cenomonian-Turonian exposures in West-Central Sinai (Egypt); *Revue de Micropaleontology* 31, 243-262.
- Colombie. C., Strasser, A., 2005. Facies, cycles, and controls on the evolution of a keep-up carbonate platform (Kimmeridgian, Swiss Jura), *Sedimentology* 52, 1207–1227.
- Davies P. J., Symonds P.A., Feary D. A., Pigram C. J., 1989. The evolution of the carbonate platforms of northeastern Australia. In: Crevello P.D., Wilson J. L., Sarg J. F., Read J. F. (Eds.). *Controls on carbonate platform and basin development*. Society Economic Paleontologists Mineralogists, Special Publication 44, 233– 258.

- Drzewiecki, P. A., Simo, J. A. T., 1997. Carbonate platform drowning and oceanic anoxic events on a mid- Cretaceous carbonate platforms, south-central Pyrenees, Spain. *Journal of Sedimentary Research* 67, 698-714
- Drzewiecki, P. A., Simó, J. A., 2000. Tectonic, eustatic and environmental controls on Mid-Cretaceous carbonate platform, south central Pyrenees, Spain: *Sedimentology* 47, 471-495.
- Einsele, G. ,1992. *Sedimentary basins*. Berlin7 Springer Verlag.
- El-Azabi, M. H. and El-Araby. A., 1996. Depositional facies and paleoenvironments of Albian - Cenomanian sediments in Gebel El-Minsherh, north central Sinai, Egypt.- *Geological Society of Egypt, Special Publication* 2, 151-198. Cairo.
- El-Azabi, M.H. and Farouk, S. 2011. High-resolution sequence stratigraphy of the Maastrichtian-Ypresian succession along the eastern scarp face of the Kharga Oasis, south Western Desert, Egypt. *Journal International Association Sedimentology*, 58, 579–617.
- El Emam, A., Dishopp, D., Dunderdale, I., 1990. The structural setting of the central Western Desert, Egypt. In: *Proceedings of the 10 th Egyptian General Petroleum Corporation Seminar* 2, 30–70
- El Shinnawi, M.A. ; Sultan, I. Z., 1972. Biostratigraphy of some Upper Cretaceous sections in the Gulf of Suez area, Egypt. *Proceeding of 5th Colloquium African micropaleontology*, p. 263-29.

- El-Hariri, T., Mousa, A., Moustafa, T., Farouk, S. 2012. Facies and sedimentary environments of the Abu Qada Formation at Gabal El-Gunna, Southeastern Sinai, Egypt. *Egyptian Journal of Petroleum*, 21, 71–79.
- Elrick, M. and Read, J. F., 1991. Cyclic ramp to basin carbonate deposits, Lower Mississippian Wyoming and Montana; A combined field and computer modeling study; *Journal Sedimentary Research* 61, 1194-1224.
- Farouk, S. 2015. Upper Cretaceous sequence stratigraphy of the Galala Plateaux, western side of the Gulf of Suez, Egypt. *Marine and Petroleum Geology*. 60, 136-158.
- Farouk, S., Ahmad, F., Powell, J., Marzouk, A. 2016. Integrated microfossil biostratigraphy, facies distribution and depositional sequences of the upper Turonian to Campanian succession in northeast Egypt and Jordan. *Facies*. 62:8
- Farouk, S., Faris, M., 2012. Late Cretaceous calcareous nannofossil and planktic foraminiferal bioevents of the shallow-marine carbonate platform in Mitla Pass, west central Sinai, Egypt. *Cretaceous Research*, 33, 50-56.
- Farouk, S., Marzouk, A.M., Fayez, A., 2014. The Cretaceous / Paleogene boundary in Jordan. *Journal of Asian Earth Sciences*. 94, 113–125.
- Flügel, E., 1982. *Microfacies analysis of limestone*; Springer Verlag, Berlin, Heidelberg, New York, 631 p.
- Flügel, E., 2004. *Microfacies of carbonate rocks: analysis, interpretation, and application*. Springer, Berlin, p 976

- Folk, R.L., Land, L. S., 1975. Mg/Ca ratio and salinity: Two controls over 713
recrystallization of dolomite; American. Association Petroleum Geologists 714
Bulletin, 59: pp. 68. 715
- Friedman, G. M., 1968. The fabric of carbonate cement and matrix and its 716
dependence on the salinity of water. In: Muller, G. and Friedman, G. M. 717
(Eds.); Recent development in carbonate sedimentology in central Europe; 718
N.Y. Springer verlag, 225p. 719
- Garfunkl, Z., 1999. History and paleogeography during the Pan- African 720
orogen to stable platform transition: Reappraisal from the evidence from Elat 721
area and the northern Arabian-Nubian Shield. Israel Jour. of Earth Sciences 722
48, 135-157. 723
- Ghorab, M.A., 1961. Abnormal stratigraphic features in Ras Gharib oil field; 724
3rd Arab Petroleum congress, Alexandria, 2: 1- 10. 725
- Ginsburg, R. N., 2001. Subsurface geology of a prograding carbonate 726
platform; results of the Bahama Drilling Project. Society of Economic 727
Paleontologists Mineralogists, Special Publication; 70. [Tulsa, USA]. 728
- Gillespie, P. A., Walsh, J. J., Watterson, J., 1992. Limitations of dimension 729
and displacement data from single faults and the consequences for data 730
analysis and interpretation: Journal of Structural Geology 14, 1157–1172 731
- Guiraud, R.; Issawi, B.; Bosworth, W., 2001. Phanerozoic history of Egypt 732
and surrounding areas. In: Ziegler, P. A., Cavazza, W.; Robertson, A.H.F. 733
and Crasquin-Soleau, S. (Eds.), Peri-Tethys Memoir 6: Peri-Tethyan 734

Rift/Wrench Basins and Passive Margins. Memoir Musum History Nature,	735
469-509. Paris.	736
Hayton, S., Nelson, C. S., Hood, S. D., 1995. A skeletal assemblage	737
classification system for non-tropical carbonate deposits based on New	738
Zealand Cenozoic limestones. <i>Sedimentary Geology</i> 100, 123-141.	739
Henson, F. R. S., 1950. Cretaceous and Tertiary reef formations and	740
associated sediments in the Middle East. <i>American Association Petroleum</i>	741
<i>Geologists Bulletin</i> 34, 215-238.	742
Ismail, A. A., 2000. Upper Cretaceous stratigraphy and micropaleontology of	743
the western part of the Gulf of Aqba, East Sinai, Egypt. <i>Middle East Research</i>	744
<i>Center, Ain Shams University, Earth Science Series</i> 14, 239–261.	745
Issawi, B., El. Hinnawi, M., El-Khawaga, E., Labib, S., Anani, N. 1981.	746
Contribution to the geology of Wadi Feiran area, Sinai, Egypt, <i>Geol. Survey</i>	747
<i>Egypt, Internal Report</i> , 1-43.	748
James, N.P., Kendall, A. C., 1992. Introduction to carbonate and evaporite	749
facies models. - In: Walker. R.G. (Ed.): <i>Facies models: response to seal-level</i>	750
<i>changes. Geological Association of Canada</i> , 265-275	751
Jenkins, D., 1990. North and central Sinai. In: Said, R. (Ed.), <i>The Geology of</i>	752
<i>Egypt</i> , pp. 361–380. Balkema, Rotterdam.	753
Kaźmierczak, J., 1975. Colonial Volvocales (Chlorophyta) from the Upper	754
Devonian of Poland and their paleoenvironmental significance. <i>Acta</i>	755
<i>Palaeontologica Polonica</i> 20 , 73–89.	756

- Kaźmierczak, J., 1976. Volvocacean nature of some Palaeozoic non- 757
radiosphaerid calcispheres and parathuramminid “foraminifera.”Acta 758
Palaeontologica Polonica 21, 245–262. 759
- Kazmierczak, J., Kremer, B., 2005. Early post-mortem calcified Devonian 760
acritarchs as a source of calcispheric structures. *Facies* 51, 554-565 761
- Keller, M., 1997. Evolution and sequence stratigraphy of an Early Devonian 762
carbonate Ramp, Cantabrian Mountains Northern Spain. *Journal of* 763
Sedimentary Research 67, 638–652. 764
- Keupp, H., 1981. Die kalkigen Dinoflagellaten-Zysten der borealen Unter- 765
Kreide (Unter-Hauterivium bis Unter-Albium). *Facies* 5, 1-190 766
- Khalifa, M. A., 1996. Depositional cycles in relation to sea-level changes, case 767
studies from Egypt and Saudi Arabia. *Egyptian Journal of Geology* 40,141- 768
171. 769
- Khalifa, M.A., Zaghloul, S. A., 1990. Carbonate lithofacies and depositional 770
environments of the Lower Eocene Farafra Oasis, Western Desert, Egypt. 771
Journal of African Earth Sciences 11, 281- 772
- Khalifa, M.A., Abu-El Hassan, M.M., 1993. Lithofacies, cyclicity, diagenesis 773
and depositional environments of the Upper Cenomanian, El Heiz Formation, 774
Bahariya Oasis, Western Desert, Egypt, *Journal African Earth Sciences* 17 , 775
555-570. 776
- Khalifa, M. A, Askalany, M. M., Seleim, M. M., 2003. Lithofacies and 777
depositional environments of the Cenomanian Galala Formation and Early 778

- Turonian Abu Qada Formation, Central Western Sinai, Egypt. *Annals. Geological Survey, Egypt* XXVI, 217-234. 779 780
- Klein G. Dev., 1970. Tidal origin of a Precambrian quartzite. The lower fine-grained quartzite (Middle Dalradian) of Islay-Scotland. *Journal of Sedimentary Petrology* 40, 973–998 781 782 783
- Kora, H., Hamama, H., 1987. Biostratigraphy of the Senonian succession in Bir Safra area, Southeastern Sinai, Egypt, *Mars. Sci. Bull.*, 14(2): 303-314. 784 785
- Kuss, J., Scheibner, C., Gietl. R., 2000. Carbonate platform to basin transition along an Upper Cretaceous to Lower Tertiary Syrian Arc uplift, Galala Plateaus, Eastern Desert, Egypt. *GeoArabia* 5, 405-424, Bahrain. 786 787 788
- Luning, S., Kuss, J., Bachmann, M., Marzouk, A. M. ; Morsi, A. M. ,1998a Sedimentary response to basin inversion: Mid Cretaceous - Early Tertiary pre- to syndeformational deposition at the Areif El Naqa anticline (Sinai, Egypt)- Facies, 38,103-136, Erlangen. 789 790 791 792
- Luning, S., Marzouk, A.M., Morsi, A.M., Kuss, J., 1998b. Sequence stratigraphy of the Upper Cretaceous of central-east Sinai, Egypt. *Cretaceous Research* 19, 153–196. 793 794 795
- Machel, H. G., Anderson, J. H., 1989. Pervasive subsurface dolomitization of the Nisku Formation in central Alberta: *Journal of Sedimentary Petrology* 59, 891- 911. 796 797 798
- Mack, G. H., James, W. C., 1986. Cyclic sedimentation in the mixed siliciclastic-carbonate Abo-Hueco transitional zone (Lower Permian), southwestern New Mexico. *Journal Sedimentary Petrology* 56, 635-647. 799 800 801

- Markello, J. R., Read, J. F., 1981. Carbonate ramp-to-deep shale shelf 802
transitions of an Upper Cambrian intrashelf basin, Nolichucky Formation, 803
southwest Virginia Appalachians. *Sedimentology* 2, 573–597. 804
- Marszalek, D. S., 1975. Calcsphere ultrastructure and skeletal aragonite from 805
the algae *Acetabularia antillana*. *Journal of Sedimentary Petrology* 45, 266– 806
271. 807
- Marquis, S.A., Laury, R.L., 1989. Glacio-eustasy, depositional environment, 808
diagenesis and reservoir character of Geon Limestone Cyclothem 809
(Desmoinesian), Concho platform, central Texas. *American Association of* 810
Petroleum Geologists Bulletin 73, 166–181. 811
- Moustafa, A.R., Khalil, M.H. 1990. Structural characteristics and tectonic 812
evolution of north Sinai fold belts: In R. Said (Ed.), *Geology of Egypt*, A. A. 813
Balkema, Rotterdam, Brookfield, pp. 381–389 814
- Nelson, C. S., Keane, S. I.; Head, P. S., 1988. Non-tropical carbonate deposits 815
on the modern New Zealand shelf. *Sedimentary Geology* 60, 71-94. 816
- Osleger D, Read J.F., 1991. Relation of eustasy to stacking patterns of meter- 817
scale carbonate cycles, Late Cambrian, USA. *Journal Sediment Petrology* 61, 818
1225–1252 819
- Peryt, T. M., 1977. Environmental significance of foraminiferal algal 820
oncolites: In: Flugel, E. (Ed.) *Fossil Algae, Recent Results and* 821
Developments. Springer-Verlag, Heidelberg, 375 p. 822

- Philip, J., Airaud-Crumière C., 1991. The demise of the rudistbearing 823
carbonate platforms at the Cenomanian/Turonian boundary: a global control. 824
Coral Reefs 10, 115-125. 825
- Philip, J., Borgomano, J., Al-Maskiry, S., 1995. Cenomanian-Early Turonian 826
carbonate platform of northern Oman; stratigraphy and palaeo-environments. 827
Palaeogeography Palaeoclimatology Palaeoecology 119, 77-92. 828
- Potter, P. E., Maynard, J. B., Pryor W. A., 1980. Sedimentology of Shale. 829
Springer, New York, p 306 830
- Sadler, P. M., Osleger, D. A. and Montanez, I. P., 1993. On the labeling, 831
length and objective basis of Fischer plots. Journal of Sedimentary Petrology 832
63, 360-368. 833
- Said, R. 1962. The geology of Egypt; Elsevier, Amsterdam-Oxford- New 834
York, 337 p. 835
- Said, R., 1971. Explanatory Note to Accompany the Geological map of Egypt, 836
Geological Survey of Egypt. Paper (56,) 123 p. 837
- Salem, A. M. K., Abdel Wahab, A. McBride, E. F. 1998. Diagenesis of 838
shallowly buried cratonic sandstones, southwest Sinai, Egypt. Sedimentary 839
Geology 119, 311-335. 840
- Samuel, M. D., Ismail, A.A., Akarish, A. I. M., Zaky, A. H., 2009. Upper 841
Cretaceous stratigraphy of the Gebel Somar area, north-central Sinai, Egypt. 842
Cretaceous Research 30, 22-34. 843
- Shahar, J., 1994. The Syrian Arc system: an overview. Palaeogeography 844
Palaeoclimatology Palaeoecology 112, 125-142 845

- Shinn, E.A., Ginsburg, R. N.; Lloyd, R. M., 1965. Recent supratidal dolomite 846
 from Andros Island, Bahamas. In: Pray, L. C., Murray, R.C. (Eds.), 847
 Dolomitization and Limestone Diagenesis: Society of Economic 848
 Paleontologists and Mineralogists Special Publication 13, 112-123. 849
- Schlager, W., 1981. The paradox of downward reefs and carbonate platforms. 850
 Geological Society of American Bulletin 92, 197-211. 851
- Schlager, W., Ginsburg, R. N., 1981. Bahama carbonate platforms, the deep 852
 and the past. *Marine Geology*, 44, 1– 24. 853
- Schlager, W., 1999. Type 3 sequence boundaries. In: Harris, P.M. ; Saller, A. 854
 H., J. A. Simo, J. A. (Eds.) *Advances in Carbonate Sequence Stratigraphy:* 855
Application to Reservoirs, Outcrops and Models. Society Economic 856
 Paleontologists Mineralogists Special Publication 63, 35–45. 857
- Shahin, A., Kora, M., 1991. Biostratigraphy of some Upper Cretaceous 858
 succession in the Eastern Central Sinai, Egypt. *Neues Jahrbuch für Geologie* 859
und Paläontologie, Monatshefte 11, 671–692. 860
- Shinn, E. A., 1983. Tidal flat environment. In: Scholle P. A., Bebout D. G., 861
 Moore, C. H. (Eds.) *Carbonate depositional environments.* American 862
 Association of Petroleum Geologists Memoir 33, 171–210 863
- Sibley, D. F., Gregg, J. M., Brown, R. G.: Laudon, P. R., 1993. Dolomite 864
 crystal size distribution, In: Rezak, R., Lavoie, D. L. (Eds.), *Carbonate* 865
Microfabrics: Springer-Verlag, New York, p. 195-204. 866
- Stern, R. J., 1985. The Najd fault system, Saudi Arabia and Egypt. A late 867
 Precambrian rift-related transform system. *Tectonics* 4, 497–511. 868

- Szulezewski, M. Belka. Z., Skompski, S., 1996. The drowning of a carbonate platform: an example from the Devonian-Carboniferous of the southwestern Holy Cross Mountains. *Sedimentary Geology* 106, 21-49.
- Tucker ME, Wright VP (1990) *Carbonate sedimentology*. Blackwell Scientific Publication, Oxford, p 49
- Tucker, M. E., Calvet, F., Hunt, D., 1993. Sequence stratigraphy of carbonate ramps: Systems tracts, models and application to the Muschelkalk carbonate platforms of eastern Spain. In: Posamentier, H.W., Summerhayes, C.P., Haq, B.U., Allen, G.P. (Eds.), *Sequence Stratigraphy and Facies Associations*. International Association of Sedimentologists Special Publication 18, Blackwell, Oxford, pp. 397.
- Walley, C.D., 1998. Some outstanding issues in the geology of Lebanon and their importance in the tectonic evolution of the Levantine region. *Tectonophysics* 298, 37-62.
- Wilmsen, M., Nagm, E., 2012. Depositional environments and facies development of the Cenomanian–Turonian Galala and Maghra el Hadida formations of the Southern Galala Plateau (Upper Cretaceous, Eastern Desert, Egypt). *Facies* 58, 229–247.
- Wilson, J. L., 1975. *Carbonate facies in geologic history*. Springer Verlag, 470 p.
- Wright, V. P., Burchette, T. P., 1999. Shallow-water carbonate environments. In: Reading, H.G. (Ed.), *Sedimentary Environments: Processes, Facies and Stratigraphy*. Blackwell, Oxford, 688 p.

Ziko, A., Darwish, M. ; Eweda, S., 1993. Late Cretaceous- Early Tertiary 892
stratigraphy of the Themed area, East Central Sinai, Egypt; Neues Jahrbuch 893
für Geologie und Paläontologie, Monatshefte H.3, Stuttgart; 135-149. 894

895

Figures Captions. 896

897

Fig. 1: Location and geological map of the Sinai showing the location of the 898
studied sections of the Wata Formation. 899

Fig. (2): Lithostratigraphic correlation chart of the Wata Formation at the east 900
central Sinai, showing its, lateral, vertical facies associations, and thickness 901
variations (horizontal distance not to scale). 902

Fig. (3A): Field photograph showing the thin-bedded limestone of the Wata 903
Formation, forming the inter-platform along Sudr El-Haitan Plateau. The 904
outcrop is 200 m long. Photograph is looking north-east. 905

Fig (3B): Field photograph showing the massive limestone rich in sponges, 906
characterizing the upper part of the Wata Formation, Sudr El-Haitan. 907

Fig. (3C): Field photograph showing the massive carbonate deposits of the 908
Wata Formation (60 m thick) that unconformably overlies and underlies the 909
Abu Qada and the Matulla formations, respectively, cropping out at Ekma 910
Plateau. 911

Fig. 4A): A- Photomicrograph showing fine dense and dark grey 912
microcrystalline calcite that contains rare foraminiferal skeletal particles 913
floating in the dense lime-mud, Lime-mudstone lithofacies, Wadi Hegni. 914

Fig. 4B): Photomicrograph of the molluscan bioclastic packstone that made up of sorted molluscan particles and showing preferred orientation parallel to the bedding plane. Most of the molluscan particles exhibit aggrading neomorphism from their centers and coated with micrite envelopes, Molluscan bioclastic packstone lithofacies, Wadi Hegni.

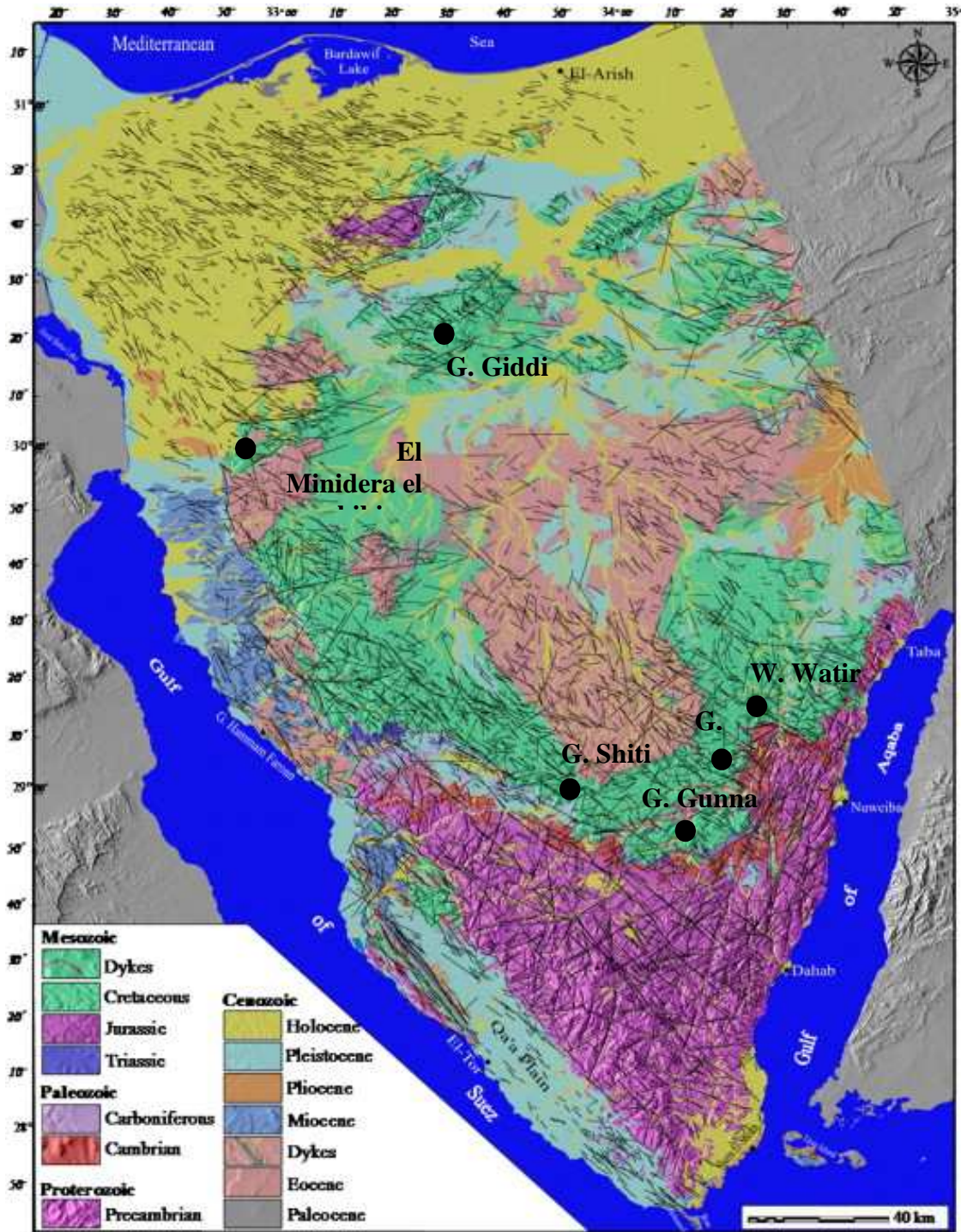
Fig. 4C): Photomicrograph of the ostracodal wackestone that comprises ostracodes and peloids embedded in lime-mud matrix. Notice the partial dolomitization of the lime-mud and the peloids, producing fine-grained idiopic to hypidiopic dolomite crystals, Ostracodal wackestone lithofacies, El Tih scarp (Gebel Shiti, Gebel Gunna, Gebel Hazim and Wadi Watir).

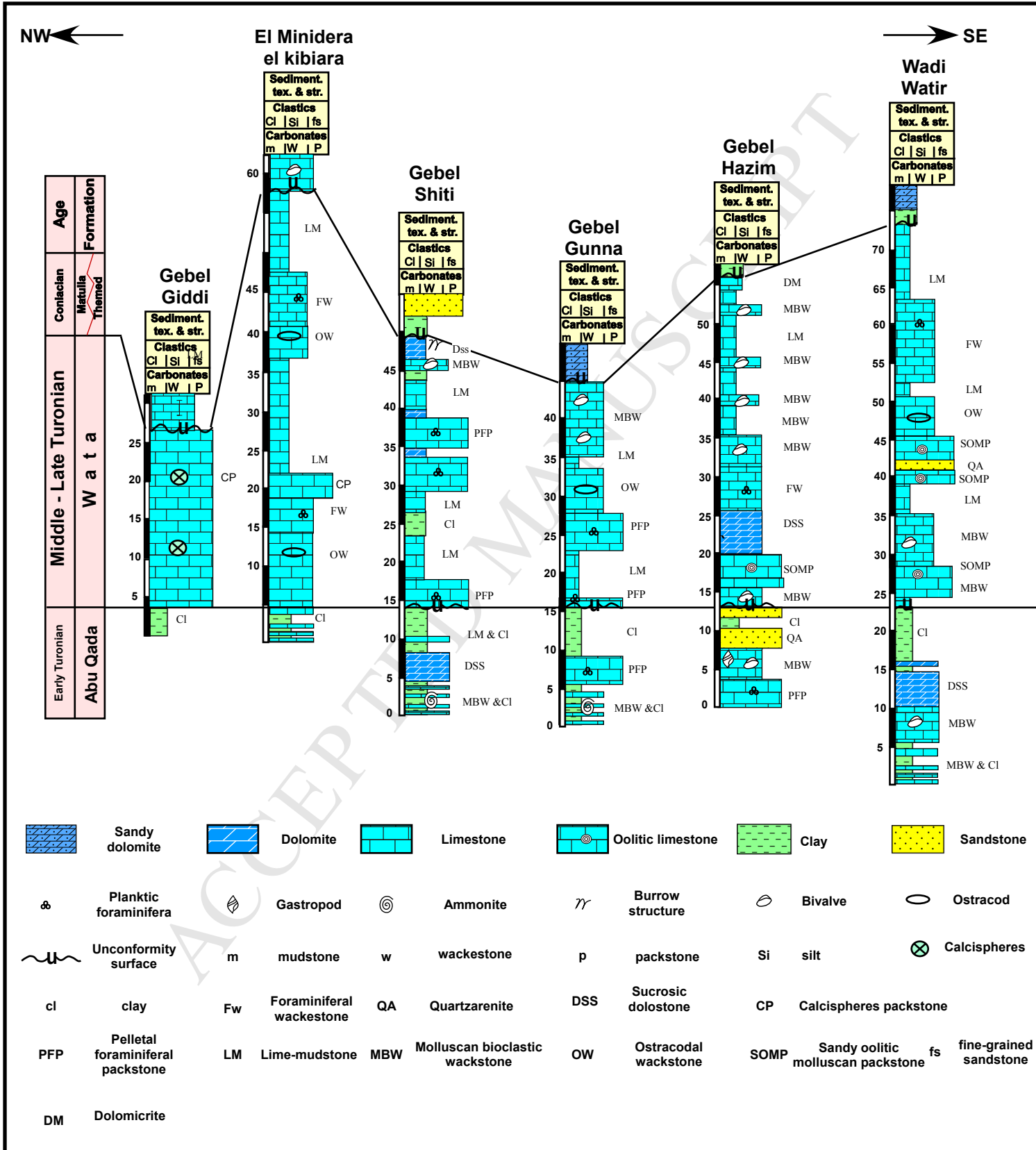
Fig. 4D): Photomicrograph showing foraminiferal wackestone in which some tests (*Heterohelix* spp.) are scattered in a lime-mud matrix with association of bioclasts and pellets, Foraminiferal wackestone lithofacies, Wadi Watir.

Fig. 5A): Photomicrograph showing the pelletal foraminiferal packstone lithofacies that consists of benthonic foraminifera and rounded to ovoided pellets, embedded in lime-mud matrix. Notice the relics of miliolid partly still preserved within the pellets, El Tih scarp (Gebel Shiti, Gebel Gunna, Gebel Hazim and Wadi Watir).

Fig. 5B): Photomicrograph showing the sandy oolitic molluscan packstone lithofacies that consists of oolites, echinoid stems and shell debris. Notice the aggrading neomorphism of the lime-mud matrix and the syntaxial calcite overgrowth around echinoids, Wadi Hegni.

- Fig.5C): Photomicrograph of the calcisphere packstone, in which the calcispheres are round to spherical with association of spongy spines and debris of bioclasts, Calcispheres packstone, Gebel Giddy and El Mineidra El Kebira.
- Fig. 5D): Photomicrograph of the dolosparite lithofacies that consists of well-defined dolomite rhombs and some unfilled pore spaces. Most of the dolomite rhombs are of medium-grained (0.08 mm) and show hypidiotopic to xenotopic fabric and equigranular texture. Notice some ferrugination cutting along cracks, El Tih scarp (Gebel Shiti, Gebel Gunna, Gebel Hazim and Wadi Watir).
- Fig. 6A): Photomicrograph of the dolomicrite that consists mainly of very fine dolomite rhombs as well as some detrital quartz grains. Dolomite rhombs are interlocked together usually lacking zoning and exhibit hypidiotopic to xenotopic with equigranular texture, Wadi Hegni (Gebel El Hazim).
- Fig. 6B): Photomicrograph of the quartzarenite that comprises compact, rounded to subrounded, medium- to coarse-grained quartz grains, Wadi Watir.
- Fig. 7A): A schematic diagram showing the possible lateral facies changes and the subdivisions of the platform of the Wata Formation.
- Fig. 7B): Schematic diagram showing the depositional environments of the inner-, inter- and outer-platforms of the Wata Formation in Sinai Peninsula in northwest-southeast direction.







3A

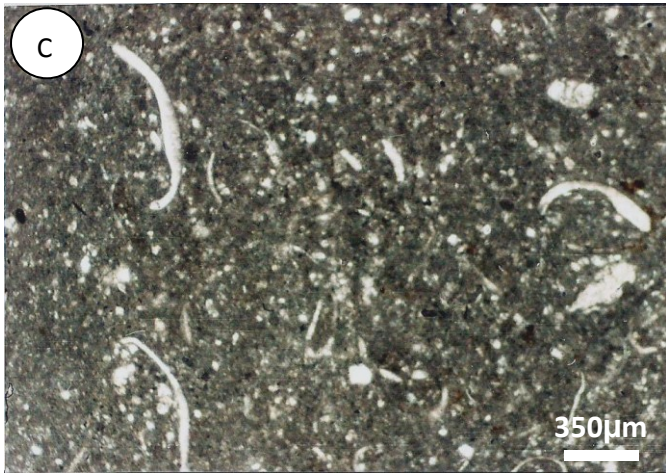
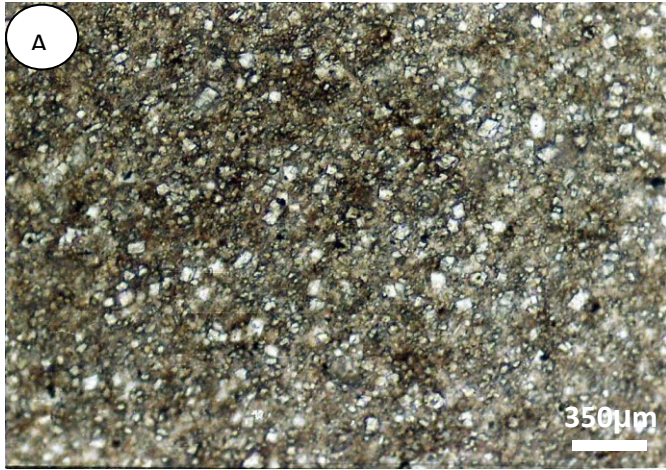


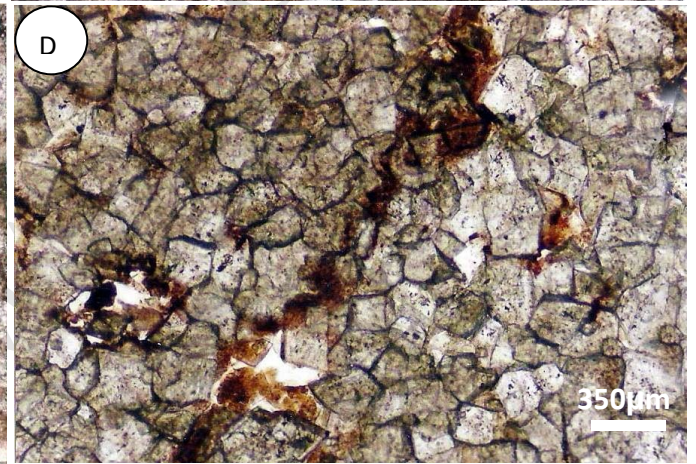
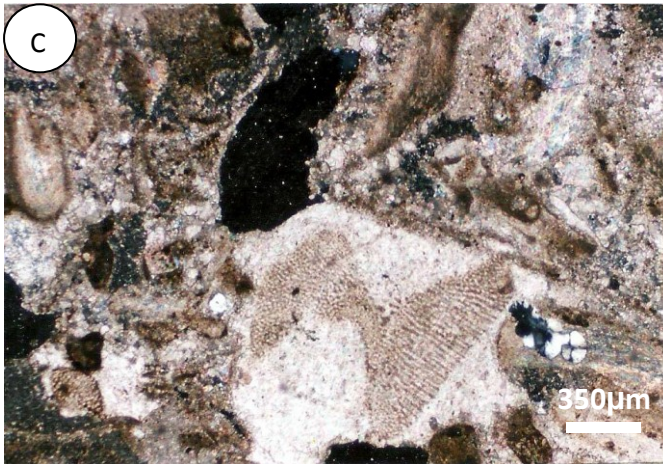
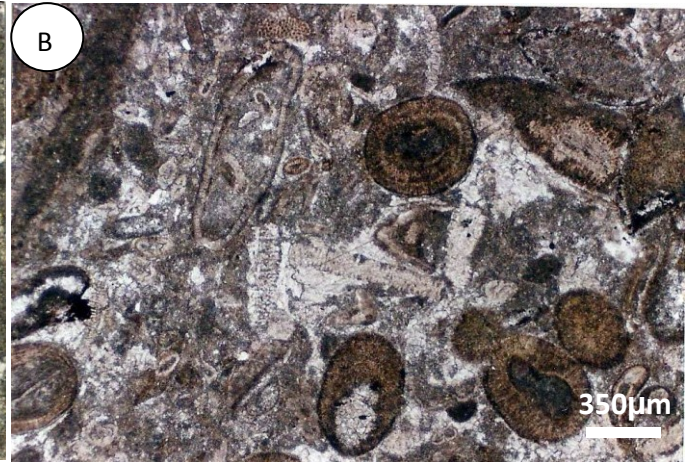
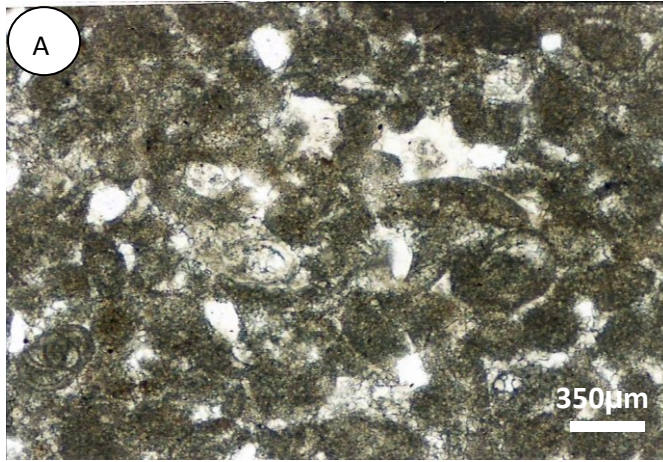
3B



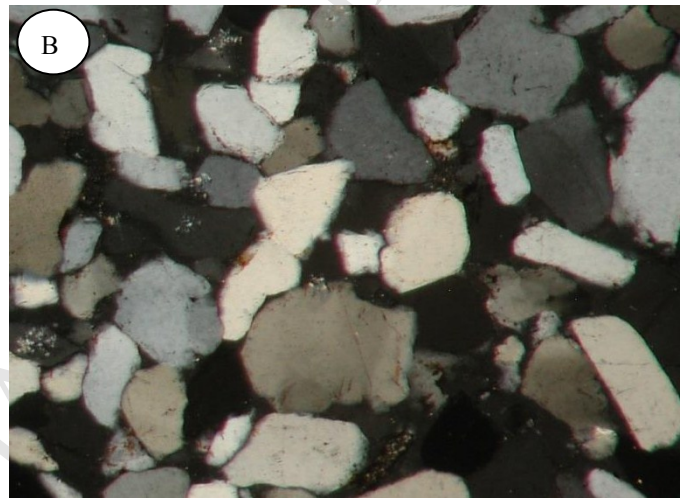
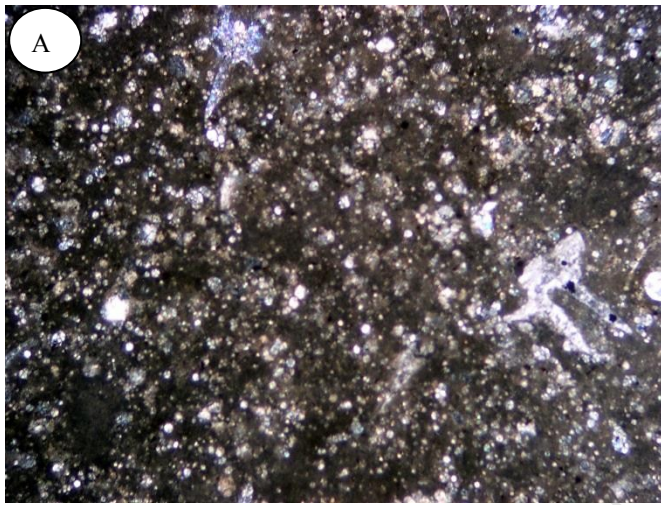
3C

ACCEPTED MANUSCRIPT





ACCEPTED



350 μm

Facies analysis of the Turonian Wata platform in Sinai.

Wata platform is classified into Inner-platform, inter-platform, outer-platform.

Different lithofacies associations have been deduced in each platform type.

Platform classification was probably performed by the effect of Syrian Arc System.

Deepening platform of the Wata Formation is based on the fining-upward cycles.